

Supporting Information

A self-contained acoustofluidic platform for biomarker detection

Xian Chen, Chuanchao Zhang, Bohua Liu, Ye Chang, Wei Pang, Xuexin Duan

State Key Laboratory of Precision Measuring Technology & Instruments and College of Precision Instrument and Opto-electronics Engineering, Tianjin University, Tianjin 300072, China

Supporting Information Video S1

The PBS buffer and blue ink were triggered into the microchannel sequentially by the external pumping accessory with the flow rate of 2 $\mu\text{L}/\text{min}$. Once the LWR was turn on (25.12 mW applied), the liquid was pushed out of the microchannel immediately and kept on the inlet. Besides, the liquid could be continuously pumped when the LWR was turn off.

Supporting Information Video S2

Under the actuation of LWR (63 mW applied), the diluted blue ink in the right inlet of vertical microchannel was drawn into microchannel, flowed towards the lower ends, and gradually filled the open chamber.

Supporting Information Video S3

The flowing particles were gradually dynamically trapped by the two acoustic micro-vortices of LWR (100 mW applied) near the inlet; after the uniform mixing based on the LWR, the formed complexes were released from the acoustic streaming and statically concentrated by the permanent along the side for the signal detection.

S1. The acoustic pressure distribution of LWR in the microchannel

When the RF power is applied on LWR, the Lamb wave could be excited in the bulk medium *via* the inverse piezoelectric effect, and subsequently propagates from the center of resonator to the sides. Besides, the cylindrical-shaped acoustic pressure distribution in both sides is formed in the liquid surroundings. What's more, the influence of microchannel size on the pressure distribution was explored when the RF power was fixed at 45 mW. As shown in Fig. S1b, the width (W) of channel was varied from 450 to 150 μm , while the height (H) was set as 85 μm . The related simulation results demonstrated that the acoustic pressure in the liquid region distributed only near the electrodes even if the width was changed. Therefore, the area unaffected by the acoustic pressure would be increased when the channel is widened. Similarly, the acoustic pressure distribution was not influenced by the height of microchannel (Fig. S1c), and the higher area was less affected by the pressure. This indicates that the microchannel size should be properly regulated to match the fluid control demand.

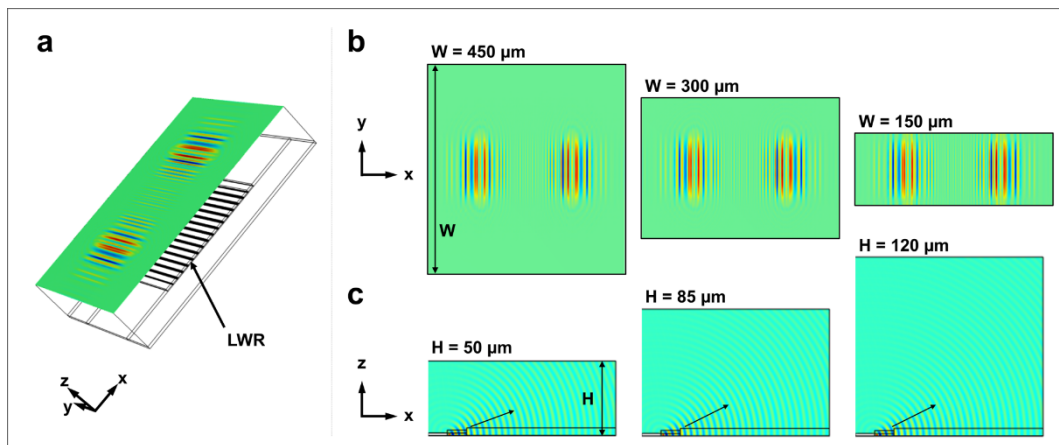


Fig. S1 (a) The simulated acoustic pressure distribution of x-y plane in the three-dimensional model when the width of microchannel was 300 μm ; (b) the acoustic pressure of x-y plane when the width was varied from 450 to 150 μm ; (c) the acoustic pressure of x-z plane when the height was varied from 50 to 120 μm .

S2. The fluid pumping of LWR in the microchannel

Herein, the PBS buffer was utilized for the demonstration of on-chip pumping based on LWR. While the acoustic resonator was placed in the vertical corner of the microchannel, the liquid in the right inlet was dragged into the channel and exited from the lower outlet. The photographs of the inlet and outlet corresponding to different time points were shown in Fig. S2.

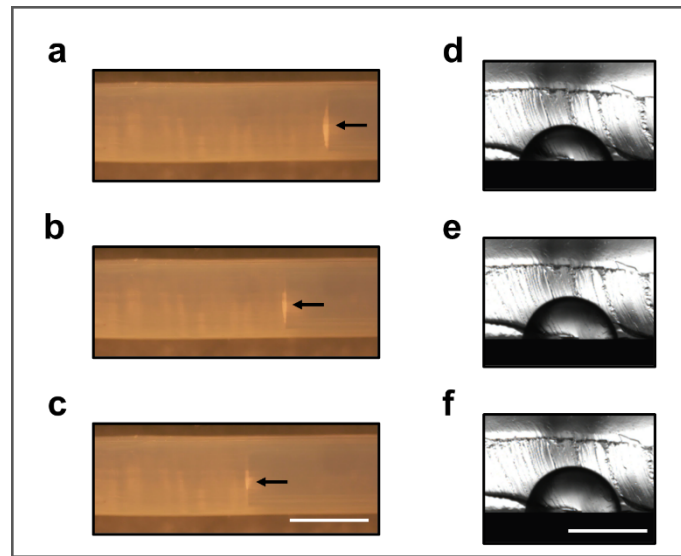


Fig. S2 The photographs captured by the microscope during the unidirectional acoustic pumping of PBS buffer in the inlet (a-c) and in the outlet (d-f). The scale bar is 1 mm.

S3. The pumping performance of LWR in the liquid with different viscosity

To illustrate the performance of device in high viscosity liquid, we prepared the liquid with different viscosity by mixing serum with PBS buffer at different ratio. The RF power of LWR was fixed at 100 mW, and the pumping flow rates in the different liquid were shown in Fig. S3. The results demonstrated that the acoustic device could realize the on-chip pumping in the liquid with a range of viscosity, while the high viscosity liquid would weaken the performance. Therefore, a higher applied power is required to realize the same performance in the high viscosity liquid.

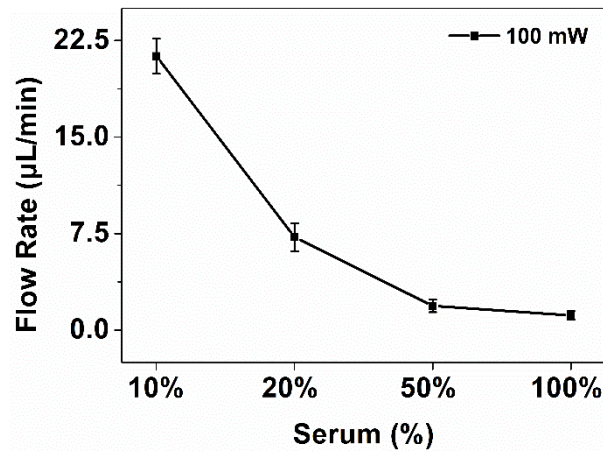


Fig. S3 The acoustic pumping flow rate in the liquid with different viscosity (10%, 20%, 50%, 100% serum).

S4. The fluid mixing of LWR in the microchannel

To demonstrate the mixing performance of LWR, the typical biotin-streptavidin (biotin-SAv) bioreaction was adopted and conducted in the microchannel. The biotin-functionalized polystyrene magnetic particles (PSM-biotin) were injected into the channel and followed by the Cy3-labeled streptavidin (SAv-Cy3). When the LWR was turned off, the PSM-biotin were directly trapped by the magnet along the boundary, and the subsequent SAv-Cy3 molecules could only react with the PSM-biotin distributed in the surface of particle clusters, which resulted in weak fluorescent light. However, the phenomenon was obviously ameliorated by applying power on LWR. When the LWR was turned on, the PSM-biotin was dynamically trapped in the two acoustic vortices near the inlet and could fully contact and react with the SAv-Cy3; then, the formed complexes were released from the LWR and statically concentrated by the magnet for the photograph capture. The related fluorescent images (Fig. S3) verified the mixing merits of LWR for bioreaction in the confined microchannel.

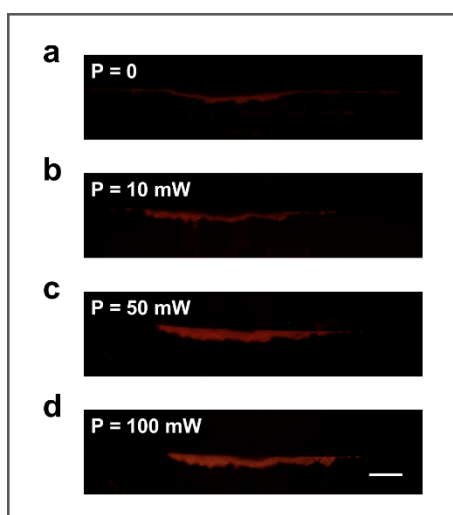


Fig. S4 Fluorescent photographs when the applied power of LWR was 0 (a), 10 (b), 50 (c), and 100 mW (d). The scale bar is 150 μm .

S5. The microfluidic chip fabrication process

The fabrication process of the PDMS microchannel is dedicatedly designed for the CMOS sensor integration and noise reduction. Firstly, the negative photoresist (SU-8 2025) with the thickness of 50 μm was spin coated on a silicon wafer, and then patterned by UV photolithography based on the precise structure of photomask. Next, the mixtures of PDMS monomers and curing agent (Sylgard 184) with the mass ratio of 10:1 were tardily poured over the structured wafer mold and degassed in the vacuum machine for 30 min. Notably, the mini-type glass sheet was placed upon the detection region of the microchannel and closed to the SU-8 structure directly through the gentle press of a size-matched magnet. Then, the treated silicon mold holding the mixtures in the horizontal state were cured in a drying oven at 85 $^{\circ}\text{C}$ for 90 min. Next, the magnet was firstly dug out prior to the peeling off the cured PDMS from the silicon wafer. Finally, a puncher was utilized for forming the inlet and outlet, and the CMOS optical sensor was directly placed upon the microfluidic chip for chemiluminescent signal capture. The schematic diagram of the microfluidic chip fabrication process is depicted in Fig. S5.

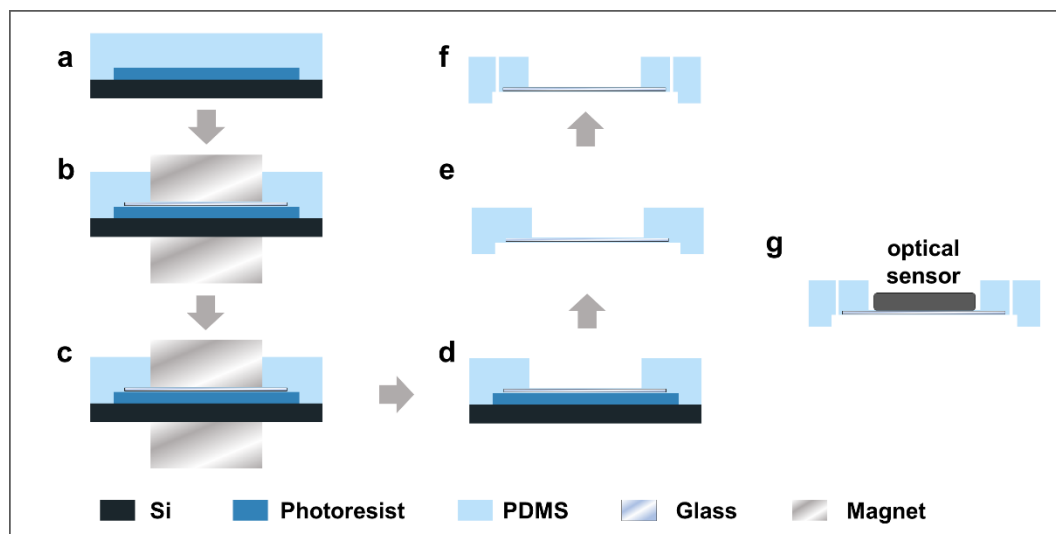


Fig. S5 The schematic diagram of microfluidic chip fabrication process: (a) adding PDMS to the structured wafer mold; (b) adding the mini-type glass sheet and the gentle press of a size-matched magnet; (c) curing the PDMS; (d) the magnet was dug out; (e) the peeling of shaped PDMS; (f) the punching based on puncher; (g) placing the CMOS optical sensor upon the microfluidic chip.

S6. Construction of the capture beads

Prior to experiments, the streptavidin-functionalized polystyrene magnetic particles (PSM-SAv) were placed into the centrifugal tube and washed by the PBS buffer for three times. Then, the biotin-labeled capture antibodies (cAbs-biotin) were added into the particle solution to construct the capture beads. After the incubation on a vortex mixer for 30 min, the formed cAbs-PSM were separated from the supernatant by a magnetic separator and rinsed with PBS buffer. Finally, the cAbs-PSM solution was stored in 4 °C refrigerator for future use.

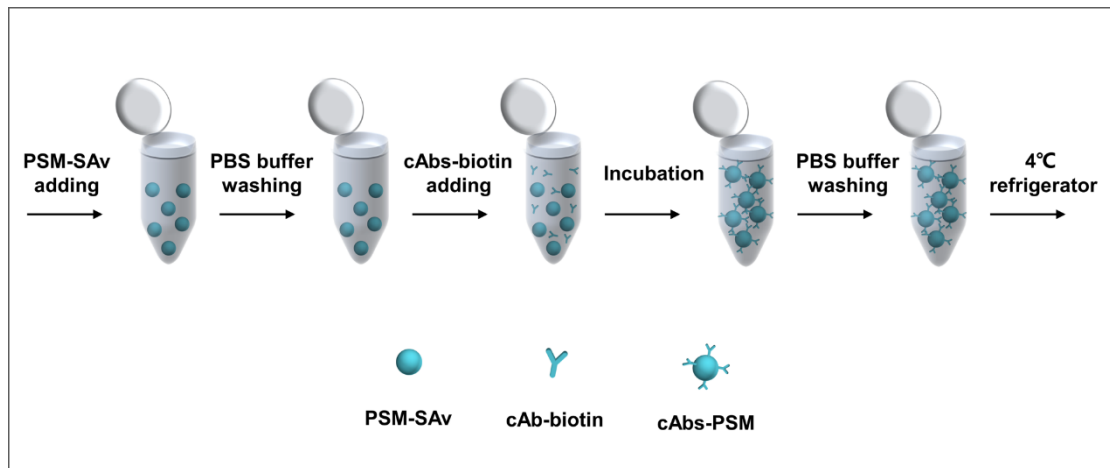


Fig. S6 Schematic diagram of the modification procedures.